LAUTECH Journal of Engineering and Technology 19 (2) 2025: 211-220
10.36108/laujet/5202.91.0222

Effects of Velocity and Battery Arrangement on Air-Cooled Lithium-ion Battery Thermal Management

[1]Adebunmi P. O., [2]Oluwasanmi I. A., [3]Ismaila O. A. and [4]Jesudetan J. A.

[1,2,3,4]*Department of Mechanical Engineering, Elizade University, Ilara-Mokin, Ondo State, Nigeria.*

[1]adebunmi.okediji@elizadeuniversity.edu.ng, [2]oluwasanmi.alonge@elizadeuniversity.edu.ng,
[3]ismaila.alabi@elizadeuniversity.edu.ng, [4]jesudetan.akinyemi@elizadeuniversity.edu.ng,

Article Info

Article history:

Received: Mar. 02, 2025
Revised: Mar. 26, 2025
Accepted: Mar. 28, 2025

Keywords:

Electric Vehicles, Li-Ion Battery, Battery Thermal Management System, Air-Cooling, Battery Arrangement

Corresponding Author:
adebunmi.okediji@elizadeuniversity.edu.ng,
+2348030527383

ABSTRACT

Thermal management of Electric vehicle (EV) batteries is essential to prevent overheating, which can lead to early battery degradation and safety risks such as thermal runaway. This study explores the impact of airflow velocity and battery arrangement on the thermal performance of air-cooled lithium-ion batteries. A Z-type battery pack was used as the battery casing, housing 15 lithium-ion batteries of 3.7-V and 3800 mAh. These batteries were arranged and connected symmetrically and asymmetrically, in both series and parallel to provide an output of 12-V and 19000-mAh. With the aid of a fan, airflow at 1, 2, and 3 m/s were supplied to the battery pack, and temperature measurements were recorded at these velocities. The symmetrical arrangement at 0 m/s under constant load had a temperature of 31.52°C, which dropped to 30.02°C, 29.87°C, and 29.22°C at 1, 2, and 3 m/s, respectively. In comparison, the asymmetrically arranged battery pack had a temperature of 30.92°C at 0 m/s, which dropped to 29.22°C, 28.87°C, and 28.57°C at 1, 2, and 3 m/s, respectively. The findings of this study can be used to improve the thermal performance, safety, and lifespan of lithium-ion batteries in various applications.

INTRODUCTION

The transportation system is one of the main causes of gasoline consumption and a significant contributor to yearly gas emissions (Chen *et al*. 2020). Over the past century, the transportation system has grown significantly. In addition to the pollution issue, the scarcity of natural resources has guided developers to increase the use of alternative technologies.

The stages toward enabling the transition to the fullest electrification of the automotive industry and transportation sector as we advance are Hybrid Electric Vehicles (HEVs) and Plug-in Hybrid Electric Vehicles (PHEVs) (Li *et al*., 2019). Today, HEVs, and PHEVs continue to face certain issues relating to the range, charging time, longevity, cost of battery price, voltage, current, and temperature range in which the batteries must operate for safety reasons and optimal performance (Li *et al*., 2020).

Due to their intrinsic temperature sensitivity, batteries can be negatively impacted by both extremely high and low temperatures. Elevated temperatures hasten deterioration, diminish capacity and longevity, and present safety hazards (Zhang and Wei 2020). On the other hand, low temperatures reduce output and impair performance (Fan *et al*., 2023). Sustaining an ideal range of operating temperatures is essential to optimize the longevity and efficiency of batteries.

Most EVs and HEVs are powered by Lithium-ion (Li-ion) batteries, which are recognized for their long life, high energy density, and efficiency. The batteries are organized in a battery pack to supply enough power for electric cars. With its

exceptional benefits of high energy density (700 Wh/L), high power factor (10000 W/L), low self-discharge rate, strong stability, and extended lifecycles in comparison to other batteries, Li-ion batteries are currently the best and most popular power source for EVs (Akhtar *et al*., 2019). However, high heat generation issues occur when high-power-density batteries are subjected to faster and more intense charging/discharging circumstances (Li *et al.*, 2020). The maximum operating temperature and temperature uniformity in electric automobiles should be restricted to 20–45 °C and 5 °C respectively, to guarantee the battery's safe and efficient operation (Zhang and Wei, 2020). When used beyond the previously indicated range, the Li-ion battery's performance rapidly deteriorates (Fan *et al*., 2023).

To keep the battery functioning without any malfunctions, battery temperature management is crucial. A Battery Thermal Management System (BTMS) uses passive cooling, active cooling, or a mix of the two to remove the heat produced in the battery pack (Dan *et al*., 2019). Using air, as a common cooling medium is the active cooling strategy (Li *et al*., 2019). The passive cooling method lowers the battery pack's temperature differential by introducing phase-change materials or heat pipes into the system (Dan *et al*., 2019). The battery's lifespan can be increased by the BTMS since it ensures that the battery pack functions under the best circumstances possible (Zang *et al*., 2018). Consequently, a great deal of work has gone into enhancing the air-cooled BTMS's cooling capabilities.

Chen *et al*. (2019) studied BTMSs with different input and output region locations to affect the airflow pattern of the BTMS and improve cooling performance. The improved BTMS reduces the maximum cell temperature differential and maximum temperature by 7.7 K and 4.5 K, respectively, as compared to the normal Z-type flow BTMS. Moreover, Hong *et al*. (2018) added a secondary vent strategically placed in a parallel air-cooled BTMS to improve the system's cooling efficiency. Placing the vent against the outlet reduced the maximum temperature differential by 60%, making it function better than BTMS without a vent.

Zang *et al*. (2022) developed an optimization approach by employing secondary outlets and baffles. The best temperature and maximum temperature difference were found to be 1.84°C and 3.66°C lower, respectively, following optimization as compared to the baseline Z-type BTMS.

In parallel air-cooled BTMS, the airflow-rate distribution among the cooling channels is determined by the cell-spacing distribution, which has a major impact on the system performance (Chen *et al*., 2019). Mohammed *et al*. (2019) experimentally investigated the air-cooling performance of aligned, staggered, and cross-battery packs. The work discovered that the system with an aligned configuration had the lowest energy consumption and the best temperature consistency.

Chen *et al*. (2019) worked on forced air-cooled BTMS for two distinct 16-cell layout techniques: square and rectangle configurations. Both configurations were subjected to thermal analysis. The work concluded that a battery pack with the same number of cells may have various temperature characteristics and that the internal temperature distribution would change when the pack's shape changed from square to rectangular.

Fan *et al*. (2023) investigated how battery spacing affected an air-cooled BTMS's ability to cool. In a simulation, the study looked at 2 mm, 3 mm, 4 mm, and 5 mm spacings. The maximum

temperature was not considerably affected by changing the battery spacing; however, a 5 mm gap resulted in a slightly greater temperature difference and worse temperature uniformity throughout the battery pack. The capacity to exchange heat was also negatively impacted by smaller spacing (2 mm). In the end, a spacing of 3 mm offers the optimal compromise between cooling efficiency and temperature uniformity.

However, despite the various studies on the cooling of BTMS to enhance its performance, there is need to investigate the influence of velocity as well as different battery arrangements. Therefore, this work studies the effects of airflow on symmetrical and asymmetrical arrangement of batteries to enhance the cooling performance of Z-type BTMS.

METHODOLOGY

Model Description

A simple model of a Z-type battery pack was created, and the lithium-ion battery cells were assembled into two battery pack configurations: (a) symmetrical, and (b) asymmetrical suitable for experimental testing. It was ensured that the battery pack incorporated an air-cooling system with carefully designed cooling channels to facilitate uniform airflow distribution. Three air velocities (1m/s, 2m/s, and 3m/s) were considered for each arrangement. The average battery pack temperature and temperature difference were used as a performance measure to evaluate, compare, and assess the system design. The overall experimental setup is shown in Figure 1.

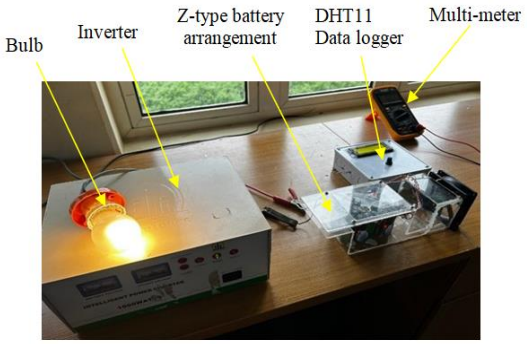

Figure 1: Experimental Set-Up

Z-type Air-Cooled BTMS Model

A Z-type battery pack shown in Figure 2 (all dimensions in mm) housing fifteen (15) cylindrical li-ion cells (12V, 19Ah) shown in Figure 3 was used. The inlet and outlet channels were placed on opposite sides of the battery pack, providing a channel for airflow. Table 1 shows the properties of the battery pack.

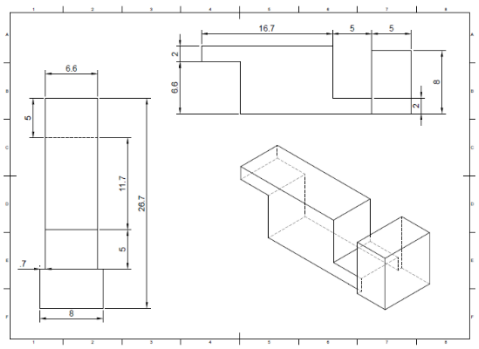

Figure 2: Schematic Diagram of Z-type casing

Figure 3: Lithium-ion battery cell

Table 1: Properties and Dimension of Battery Casing and Cell

Parameter	Value
Number of battery cell	15
Cell spacing	0.3 cm
Inlet and outlet width	6.6 cm
Inlet and outlet length	5.0 cm
Inlet and outlet height	2.0 cm
Battery cell size	6.5 cm × 1.7 cm
Model	18650
Nominal Voltage	3.7 V
Capacity	3800 mAh
Weight	0.045 kg

Components used

a) **DC Fan:** A DC fan with ratings of 12V and 0.50A is employed to generate airflow across the battery pack as shown in Figure 4. Its compact size and adjustable speed make it suitable for precise control of air velocity.

Figure 4: DC Fan

b) Temperature Sensor (DHT11): The DHT11 sensor shown in Figure 5 and its specifications as shown in Table 2, was utilized. It provides a digital output of both temperature and humidity readings. In this study, only the temperature data was utilized. The sensor's low-cost nature allows four units to be deployed at various locations within the battery pack for comprehensive temperature profiling under different experimental conditions.

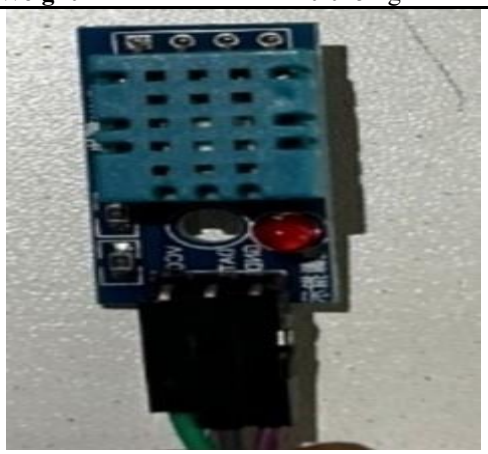

Figure 5: DHT 11 Sensor

Parameter	Value
Temperature range	0°C to 50°C with ±2°C accuracy
Humidity range	20% to 90% RH with ±5% accuracy
Sampling rate	1 Hz (one reading per second)
Output	Digital signal

Table 2: Property of DHT11

c) Arduino Board: The Arduino Uno is an open-source microcontroller board. The board includes various digital and analog

input/output pins (14 digital and 6 analog) as shown in Figure 6, allowing users to interface with temperature sensors, LEDs, switches, and other electronic components. The Arduino Uno can be powered and programmed through a USB interface, making it easy to connect to a computer for programming and communication with other devices. It also provides power options through 5V and 3.3V pins, as well as an external power input (Vin) for versatility.

Figure 6: Arduino Board

d) Field Effect Transistors (FETs): These are a type of transistor that uses an electric field to control the flow of current. They are used as switches to control the power delivered to the motor. IRF 3206 MOSFET as shown in Figure 7 was used in the study. The IRF3206 is a high-current N-Channel MOSFET that can switch currents up to 110A and 55V. These semiconductor devices are employed to modulate the voltage supplied to the DC fans, thereby regulating their speed. FETs are preferred over bipolar junction transistors (BJTs) due to their higher efficiency, faster switching speeds, lower power dissipation, and higher current handling capabilities. A FET has three main terminals: Source (S), Drain (D), and, Gate (G).

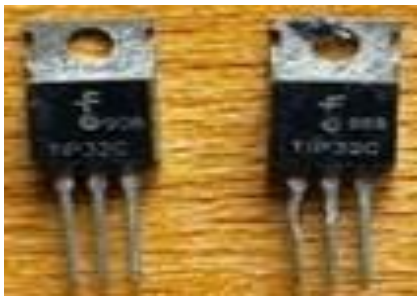

Figure 7: Field Effect Transistors (FETs)

e) Liquid Crystal Display (LCD): A 20 by 4 LCD as shown in Figure 8 was employed in this study to visualize the temperature data collected by the DHT11 sensors and the speed of the fan in real-time. This display module consists of 20 characters across 4 rows, offering ample space to present multiple temperature readings simultaneously. The LCD is interfaced with the Arduino board, which controls the displayed information.

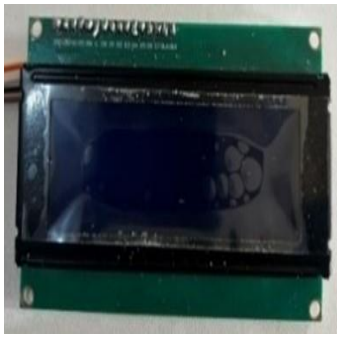

Figure 8: 20 by 4 Liquid Crystal Display

f) Heat Sink: A 0.5 ^{o}C/W heat sink as shown in Figure 9 is attached to the FETs to dissipate heat generated during operation, ensuring stable performance. It is known for its high thermal conductivity which helps dissipate heat effectively from the transistors.

Figure 9: Heat Sink

g) Potentiometer: A variable resistor was incorporated into the circuit to regulate the voltage supplied to the DC fan motor. By adjusting the potentiometer's wiper position, the resistance in the circuit changes, thereby altering the voltage and consequently, the fan speed. It was calibrated to ensure that specific resistance settings correspond to the desired airflow velocities (1 ms-1, 2 ms-1, and 3 ms-1).

h) Control Box: The control box was used as the housing for all the components of the controller including the control knob.

i) Inverter: An inverter of 1000 W shown in Figure 10 was incorporated into the experimental setup to convert the DC output of the lithium-ion battery into AC power, which was then used to operate a 60W bulb. This approach was essential for simulating real-world load conditions and inducing a controlled heat generation within the battery pack.

Figure 10: An Inverter

Assembly of Batteries

The Li-ion batteries were first soldered in series of three to give an output rating of 12V and 3,800mAh. Five sets of the series connection were made. The five sets were then connected in parallel to give an output rating of 12V and 19Ah. This was done by connecting all the positive terminals of the 5 sets and all the negative terminals. The battery set was then arranged into symmetrically or asymmetrically patterns as shown in Figures 11 and 12 respectively.

Figure 11: Symmetrical Arrangement

Figure 12: Asymmetrical Arrangement

Experimental Procedure

A 60W bulb was attached to a lamp holder and the lamp holder's output was connected to the inverter's output. The lithium-ion battery was connected to the inverter's input (positive to positive, negative to negative). The DHT11 temperature sensors were securely mounted on the battery casing and connected to the LCD data logger. The controller box was turned on, to verify that the DHT11 sensors display temperature and

humidity readings on the LCD. The initial battery casing temperature was recorded. The inverter was switched on to start the battery loading process; the bulb illuminated and generated heat over time. The battery was allowed to generate heat for 20 minutes, and the temperature readings were recorded from the LCD. The DC fan was turned on using the potentiometer knob and the speed was set to 1 m/s (verified with an anemometer). It was allowed to run for 20 minutes, and the temperature readings were recorded using a DHT11 sensor. The procedure was repeated for 2 and 3 m/s.

RESULTS AND DISCUSSION

The results of the experiment revealed significant insights into the thermal performance of lithium-ion batteries under different cooling conditions. By varying the air velocity and comparing symmetrical and asymmetrical battery arrangements, it was observed that both factors play crucial roles in managing battery temperatures. The data demonstrates how airflow and battery configuration can effectively reduce temperatures, thereby improving the overall efficiency and safety of the battery pack.

Effects of Velocity on Symmetrically Arranged Air-Cooled Lithium-Ion Batteries

Figure 13 shows the relationship between lithium-ion battery pack temperature and air velocity when the batteries were symmetrically arranged.

Due to the lack of an external cooling system, the temperature of the symmetrically organized battery pack reached its highest recorded value of 31.52°C at 0 m/s and constant loading conditions. This is a bit higher than the values reported by Yao *et al*. (2020), Zhang and Wei (2020), and Boonma *et al*. (2022), which are 24.8 °C, 25 ± 2 °C and 25 ≤ Tamb≤ 40 °C, respectively obtained under a more controlled environment.

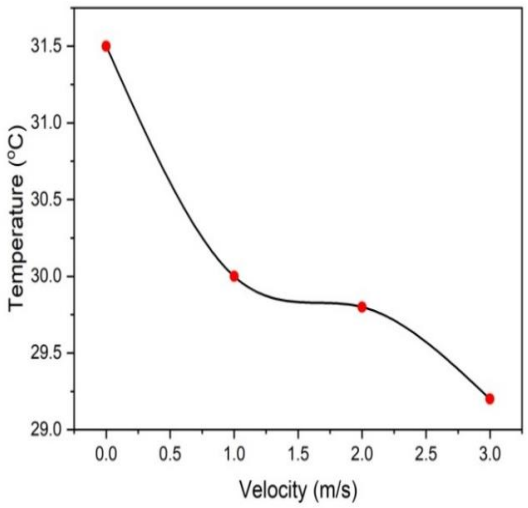

Figure 13: Graph of Temperature against velocity for Symmetrical Arrangement

The temperature dropped to about 30°C when the air velocity was raised to 1 m/s. This suggests that the cooling performance can be affected by a slight increase in air velocity above the ambient, resulting in a temperature drop (ΔT) of 1.5 °C. When the air velocity increased to 2 m/s, the temperature dropped further to 29.87°C (ΔT = 1.65°C). Although the rate of temperature drop was not as rapid as when the velocity was at 1 m/s, cooling performance was still improved. This implies that the marginal benefits of increasing air velocity tend to decline, and convective cooling was nevertheless enhanced. The temperature dropped to precisely 29.22°C (ΔT = 2.3°C) at 3 m/s. These values of temperature difference (ΔT) conform to what was reported by Yao *et al*. (2020), Zhang and Wei (2020), and Boonma *et al*. (2022) where the batteries were maintained at below 5 °C temperature difference.

The result, as shown in Figure 13 appears to have been a point of diminishing returns, where increasing air velocity further produced lesser temperature reductions, as seen by the incremental temperature drop being less noticeable than in earlier steps. The result illustrates the cooling mechanism's efficiency up to a certain point, after

which further increases in air velocity result in insignificant gains in temperature reduction.

Effects of Velocity on Asymmetrically Arranged Air-Cooled Lithium-Ion Batteries

Figure 14 shows the relationship between lithium-ion battery pack temperature and air velocity when the batteries were asymmetrically arranged.

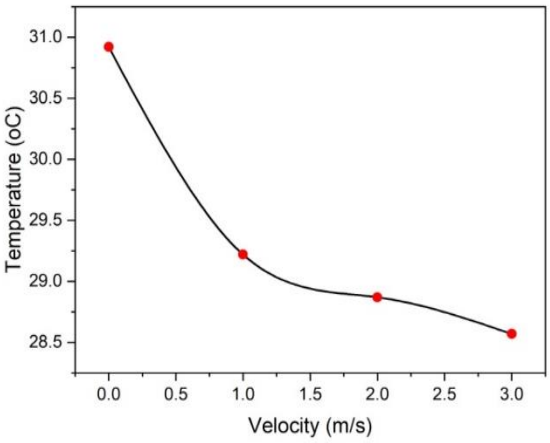

Figure 14: Graph of Temperature against Velocity for Asymmetrically Arrangement

At 0 m/s, the temperature of the asymmetrically arranged battery pack was 30.92°C under constant loading conditions. The temperature decreased to 29.22°C when the air velocity was raised to 1 m/s resulting in a temperature reduction (ΔT) of approximately 1.7°C. The moving air aided in effectively dissipating the heat produced by the batteries and contributed to the temperature drop. The battery temperature further dropped to 28.87°C (ΔT = 2.05°C) at 2 m/s air velocity. Even though this was a better cooling rate than the 1 m/s velocity, the rate of temperature reduced, suggesting that there were fewer benefits to increasing airflow. When velocity was increased to 3 m/s, the temperature dropped to 28.57°C (ΔT = 2.35°C). This implies that the cooling system's efficiency peaks and that additional air velocity further reduces temperature.

Effects of Battery Arrangement on Z-type Air-Cooled Lithium-Ion Batteries

Figure 15 presents a comparative analysis of temperature variations in symmetrically and asymmetrically arranged lithium-ion batteries within a Z-type air-cooled pack, as influenced by changes in air velocity. The x-axis denotes air velocity in meters per second, while the y-axis indicates battery pack temperature in degrees Celsius.

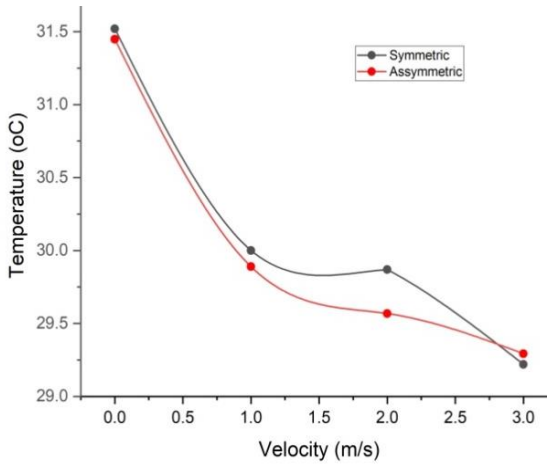

Figure 15: Comparison between Symmetrical and Asymmetrical Arrangements

Temperature reductions (ΔT) of 1.5°C in the symmetrical arrangement and 1.7°C in the asymmetrical arrangement were observed at a velocity of 1 m/s, indicating that the asymmetrical arrangement of the batteries performed better in terms of cooling than the symmetrical arrangement. Similarly, the asymmetrical layout continued to perform better in terms of cooling efficiency at a velocity of 2 m/s, as evidenced by a temperature reduction (ΔT) of 0.35°C in the asymmetrical arrangement and 0.15°C in the symmetrical arrangement. In contrast to the preceding data, the symmetrical layout performed better at cooling at a velocity of 3 m/s. It reduced temperature by 0.65 °C, whereas the asymmetrical arrangement reduced temperature by 0.3°C.

These results reveal how battery arrangement and air velocity affect thermal management, implying that the ideal configuration may change as airflow conditions change. The asymmetrical arrangements encourage more efficient heat dissipation and improved air flow distribution. The asymmetrical configuration is a better option for controlling the thermal performance of air-cooled lithium-ion batteries since it produces more effective cooling.

CONCLUSION

This research investigated the influence of velocity and battery arrangement on the thermal performance of air-cooled lithium-ion batteries. The results unequivocally demonstrate that both factors significantly impact battery temperature. Increasing airflow velocity effectively reduces battery temperature, particularly in the initial stages. However, the rate of temperature reduction diminishes as velocity increases. Asymmetrical battery arrangements consistently exhibited superior cooling performance for air velocities at 1m/s and 2m/s compared to symmetrical configurations. This suggests that the asymmetrical configuration facilitates better airflow distribution and more effective heat dissipation. The findings of this study can be used to improve the thermal performance, safety, and lifespan of lithium-ion batteries in various applications. Further, work could be done by considering complementary cooling methods such as liquid or phase change materials in case of stringent thermal requirements. In addition, the impact of different battery chemistries, cell sizes, and packaging densities on thermal performance could be investigated.

REFERENCES

Akhtar, M. S., Bui, P. T., Li, Z., Yang, O., Paul, B. J., Kim, S., Kim, J., and Kumar, A. (2019). Impact of porous Mn3O4 nanostructures on the performance of rechargeable lithium-ion battery: Excellent capacity and cyclability. Solid State Ionics,336,31–38. https://doi.org/10.1016/j.ssi.2019.03.010

Boonma K., Patimaporntap N., Mbulu H., Trinuruk P., Ruangjirakit K., Laoonual Y. and Wongwises S. (2022) A Review of the Parameters Affecting a Heat Pipe Thermal Management System for Lithium-Ion Batteries, Energies, 15, 8534. https://doi.org/10.3390/en15228534

Chen, K., Chen, Y., She, Y., Song, M., Wang, S., and Chen, L. (2020) Construction of effective symmetrical air-cooled system for battery thermal management. Applied Thermal Engineering, 166, 114679.https://doi.org/10.1016/j.applthermaleng.2019.114679

Chen, K., Wu, W., Wang, S., Wu, W.., Hong, S., and Lai, Y. (2019) A critical review of battery thermal performance and liquid-based battery thermal management. Energy Conversion and Management, 182,262–281.https://doi.org/10.1016/j.enconman.2018.12.051

Chen, K., Wu, W., Yuan, F., Chen, L., and Wang, S. (2019) Cooling efficiency improvement of air-cooled battery thermal management system through designing the flow pattern. Energy, 167, 781–790. https://doi.org/10.1016/j.energy.2018.11.011

Dan, D., Yao, C., Zhang, Y., Zhang, H., Zeng, Z., and Xu, X. (2019) Dynamic thermal behavior of micro heat pipe array-air cooling battery thermal management system based on a thermal network model. Applied Thermal Engineering, 162, 114183. https://doi.org/10.1016/j.applthermaleng.2019.114183

Fan, Y., Wang, Z., Xiong, X., Zhu, J., Gao, Q., Wang, H., and Wu, H. (2023) Novel concept design of low energy hybrid battery thermal management system using PCM and multistage Tesla valve liquid cooling. Applied Thermal Engineering, 220, 119680. https://doi.org/10.1016/j.applthermaleng.2022.119680

Hong, S., Zhang, X., Chen, K., and Wang, S. (2018) Design of flow configuration for parallel air-cooled battery thermal management system with secondary vent. International Journal of Heat and MassTransfer, 116, 1204–1212. https://doi.org/10.1016/j.ijheatmasstransfer.2017.09.092

Li, W., Garg, A., Xiao, M., Peng, X., Phung, M. L. L., Tran, V. M., and Gao, L. (2020) Intelligent optimization methodology of the battery pack for electric vehicles: A multidisciplinary perspective. International Journal of Energy Research, 44(12), 9686– 9706. https://doi.org/10.1002/er.5600

Li, W., Xiao, M., Peng, X., Garg, A., and Gao, L. (2019) A surrogate thermal modeling and parametric optimization of battery pack with air cooling for EVs. Applied Thermal Engineering, 147, 90–100. https://doi.org/10.1016/j.applthermaleng.2018.10.060

Mohammed, A. H., Esmaeeli, R., Aliniagerdroudbari, H., Alhadri, M., Hashemi, S. R., Nadkarni, G., and Farhad, S. (2019). Dual-purpose cooling plate for thermal management of prismatic lithium-ion batteries during normal operation and thermal runaway. Applied Thermal Engineering, 160, 114106. https://doi.org/10.1016/j.applthermaleng.2019.114106

Yao C., Dan D., Zhang Y., Wang Y., Qian Y., Yan Y. and Zhuge W. (2020) Thermal Performance of a Micro Heat Pipe Array for Battery Thermal Management Under Special Vehicle-Operating Conditions. Automot. Innov., 3, 317–327.

Zhang, F., Liu, P., He, Y., and Li, S. (2022) Cooling performance optimization of air cooling lithium-ion battery thermal management system based on multiple secondary outlets and baffle. Journal of Energy Storage, 52, 104678. https://doi.org/10.1016/j.est.2022.104678

Zhang, J., Kang, H., Wu, K., Li, J., and Wang, Y. (2018) The impact of enclosure and boundary conditions with a wedge-shaped path and air cooling for battery thermal management in electric vehicles. International Journal of Energy Research, 42(13), 4054–4069. https://doi.org/10.1002/er.4122

Zhang, Z., and Wei, W. (2020) Experimental and numerical study of a passive thermal management system using flat heat pipes for lithium-ion batteries. Applied Thermal Engineering, 166, 114660. https://doi.org/10.1016/j.applthermaleng.2019.114660